Rapid Communications

Taking an electron-magnon duality shortcut from electron to magnon transport

Alexander Mook,[1] Börge Göbel,[2] Jürgen Henk,[1] and Ingrid Mertig[1,2]
[1]*Institut für Physik, Martin-Luther-Universität, Halle-Wittenberg, D-06099 Halle (Saale), Germany*
[2]*Max-Planck-Institut für Mikrostrukturphysik, D-06120 Halle (Saale), Germany*

(Received 13 November 2017; published 5 April 2018)

The quasiparticles in insulating magnets are the charge-neutral magnons, whose magnetic moments couple to electromagnetic fields. For collinear easy-axis magnets, this coupling can be mapped elegantly onto the scenario of charged particles in electromagnetic fields. From this mapping we obtain equations of motion for magnon wave packets equal to those of electron wave packets in metals. Thus, well-established electronic transport phenomena can be carried over to magnons: this *duality shortcut* facilitates the discussion of magnon transport. We identify the magnon versions of normal and anomalous Hall, Nernst, Ettingshausen, and Righi-Leduc effects. They are discussed for selected types of easy-axis magnets: ferromagnets, antiferromagnets, and ferrimagnets. Besides a magnon Wiedemann-Franz law and the magnon counterpart of the negative magnetoresistance of electrons in Weyl semimetals, we predict that certain low-symmetry ferrimagnets exhibit a *nonlinear* version of the anomalous magnon Hall-effect family.

DOI: 10.1103/PhysRevB.97.140401

Introduction. The portfolio of condensed-matter physics covers a large variety of phenomena related to electrons, some of them have been known for many decades—such as Landau-level quantization [1] or the anomalous Hall effect [2–5]—and others were found in recent years—such as the chiral anomaly in Weyl semimetals [6–8]. Within a semiclassical *ansatz* these phenomena are captured by the coupled equations of motion (EOM),

$$\dot{\boldsymbol{r}} = \frac{1}{\hbar}\frac{\partial \varepsilon_{n\boldsymbol{k}}}{\partial \boldsymbol{k}} - \dot{\boldsymbol{k}} \times \boldsymbol{\Omega}_{n\boldsymbol{k}}, \tag{1a}$$

$$\hbar\dot{\boldsymbol{k}} = -|e|(\boldsymbol{E} + \dot{\boldsymbol{r}} \times \boldsymbol{B}) \tag{1b}$$

for the velocity $\dot{\boldsymbol{r}}$ of and the force $\hbar\dot{\boldsymbol{k}}$ acting on an electron wave packet [9]. $\boldsymbol{E}$ and $\boldsymbol{B}$ are electric and magnetic fields, respectively; $\varepsilon_{n\boldsymbol{k}}$ is the band energy, $\boldsymbol{\Omega}_{n\boldsymbol{k}} = i\langle\nabla_{\boldsymbol{k}} u_{n\boldsymbol{k}}| \times |\nabla_{\boldsymbol{k}} u_{n\boldsymbol{k}}\rangle$ is the Berry curvature [10,11] ($|u_{n\boldsymbol{k}}\rangle$ is the lattice-periodic part of the wave function; n is the band index), and $-|e|$ is the electron's charge.

In this Rapid Communication, we study the transport of *magnons*, the bosonic excitations of magnets, which are responsible for both spin and heat transport in magnetic insulators. Since magnons carry no electric charge, there is no force acting on a magnon wave packet in uniform electromagnetic fields. However, field gradients couple to the magnetic moment of the magnons. Concentrating on collinear easy-axis (EA) magnets, we formulate the EOM for magnon wave packets in analogy to Eq. (1) with the addition that the "charge" of the magnons can be positive as well as negative.

With the EOM for noninteracting magnons formally equivalent to those for electrons, a *duality shortcut* covers the complete family of magnon transport phenomena. We start from the established results for electronic transport and replace the effective forces as well as the distribution function to arrive at transport coefficients of magnons: This procedure captures, i.a., the magnon versions of normal and anomalous Hall, Nernst, Ettingshausen, and Righi-Leduc effects, and predicts several additional phenomena. The variation possibilities of the magnon "charge" necessitate a separate consideration of ferromagnets, antiferromagnets, and ferrimagnets.

EOM of magnon wave packets in EA magnets. The magnetic texture of collinear magnets with an EA ($\parallel \hat{\boldsymbol{z}}$) does not change when a small magnetic field $\boldsymbol{B} \parallel \hat{\boldsymbol{z}}$ is applied. However, the magnon bands $\varepsilon_{n\boldsymbol{k}}$ are modified because magnons have a magnetic moment $\mu_{z,n\boldsymbol{k}} = g\mu_{\mathrm{B}}\xi_{n\boldsymbol{k}}$ with μ_{B} as Bohr's magneton and g as the Landé factor; $\xi_{n\boldsymbol{k}}$ is dimensionless. When situated in a magnetic field gradient, the magnon experiences an electrodynamical force $\hbar\dot{\boldsymbol{k}} = -\xi_{n\boldsymbol{k}} g\mu_{\mathrm{B}} \nabla B_z$. By decomposing Bohr's magneton as $g\mu_{\mathrm{B}} = |e|X$ with $X = g\hbar/(2m_{\mathrm{e}})$ (m_{e} is the electron mass) we establish $\hbar\dot{\boldsymbol{k}} = q_{n\boldsymbol{k}}\boldsymbol{\mathcal{E}}$; $q_{n\boldsymbol{k}} = -\xi_{n\boldsymbol{k}}|e|$ is the magnon's *dual charge*, and $\boldsymbol{\mathcal{E}} = X\nabla B_z$ is the *dual electric field*.

Having introduced a dual charge, a *dual magnetic field* $\boldsymbol{\mathcal{B}}$ is found by recalling the Aharonov-Casher effect [12,13]. A neutral particle with a permanent magnetic dipole $\boldsymbol{\mu}$, which is moving with velocity $\boldsymbol{v}$, induces an electric dipole $\boldsymbol{d} = \boldsymbol{v} \times \boldsymbol{\mu}/c^2$ (c is the speed of light). It interacts with an electric field $-\boldsymbol{d} \cdot \boldsymbol{E} = \boldsymbol{v} \cdot \boldsymbol{P}$ in which $\boldsymbol{P} \equiv \boldsymbol{E} \times \boldsymbol{\mu}/c^2$ is the field's momentum [14]. By writing $\boldsymbol{P} = -|e|\xi\boldsymbol{\mathcal{A}}$ with $\xi = -1$ $(+1)$ for $\boldsymbol{\mu} \parallel \hat{\boldsymbol{z}}$ ($\boldsymbol{\mu} \parallel -\hat{\boldsymbol{z}}$), we introduce the *dual vector potential* $\boldsymbol{\mathcal{A}} = X\hat{\boldsymbol{z}} \times \boldsymbol{E}/c^2$ [14–18] and, consequently, the dual magnetic field $\boldsymbol{\mathcal{B}} = \nabla \times \boldsymbol{\mathcal{A}}$ [19].

Putting our results together, we obtain the dynamical EOM,

$$\hbar\dot{\boldsymbol{k}} = q_{n\boldsymbol{k}}(\boldsymbol{\mathcal{E}} + \dot{\boldsymbol{r}} \times \boldsymbol{\mathcal{B}}) \tag{2}$$

for a magnon wave packet in EA magnets [19] with $\boldsymbol{\mathcal{E}} = X\nabla B_z$ and $\boldsymbol{\mathcal{B}} = X(\hat{\boldsymbol{z}}\nabla \cdot \boldsymbol{E} - \partial_z \boldsymbol{E})/c^2$. It describes the force on particles, whose charge $q_{n\boldsymbol{k}}$ is band and $\boldsymbol{k}$ dependent. Equation (1a) is likewise valid for magnons; $\varepsilon_{n\boldsymbol{k}}$ and $\boldsymbol{\Omega}_{n\boldsymbol{k}}$ are the energy and Berry curvature of the one-magnon states, respectively.

Magnon transport. A magnetic-field gradient ∇B_z or a temperature gradient ∇T gives rise to a magnetic-moment (or

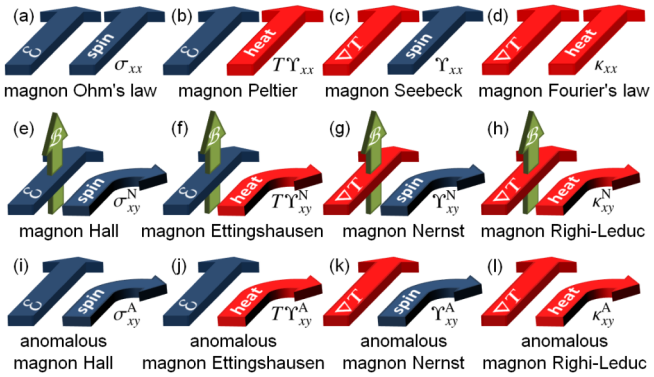

FIG. 1. Magnon transport phenomena termed according to the respective electronic counterparts. Top row, (a)–(d): longitudinal transport. Center row, (e)–(h): normal transverse transport. Bottom row, (i)–(l): anomalous transverse transport. In each panel the left (right) arrows represent the applied fields (the currents).

spin) current $\boldsymbol{J}$ and a heat current $\boldsymbol{Q}$ [20–24],

$$\boldsymbol{J} = L_0 \nabla B_z - L_1 \nabla T/T, \quad \boldsymbol{Q} = L_1 \nabla B_z - L_2 \nabla T/T. \tag{3}$$

The transport tensors L_i ($i = 0$–2) are, for example, derived in the Boltzmann approach within the relaxation-time approximation. They define the magnetization conductivity $\sigma = L_0$, the magnetothermal conductivity $\Upsilon = L_1/T$, the magnetic thermopower $S = L_0^{-1} L_1/T$, and the heat conductivity $\kappa = (L_2 - L_1 L_0^{-1} L_1)/T$.

Using Eqs. (1a) and (2), we can transfer established results of electron transport to magnon transport. Extra care is taken with regard to the particle statistics and the band-dependent charge. The longitudinal transport tensor elements read [7,19,25–27]

$$L_{i,\alpha\alpha} = \frac{(g\mu_\mathrm{B})^{2-i}}{V} \sum_{\boldsymbol{nk}} (1 + q_{\boldsymbol{nk}} \mathcal{B} \cdot \boldsymbol{\Omega}_{\boldsymbol{nk}}/\hbar)^{-1} \tau_{\boldsymbol{nk}} (-\xi_{\boldsymbol{nk}})^{2-i} \times \varepsilon_{\boldsymbol{nk}}^{i} (v_{\alpha,\boldsymbol{nk}} - q_{\boldsymbol{nk}} \mathcal{B}_\alpha \boldsymbol{v}_{\boldsymbol{nk}} \cdot \boldsymbol{\Omega}_{\boldsymbol{nk}}/\hbar)^2 \left(-\frac{\partial \rho_0}{\partial \varepsilon} \right) \Bigg|_{\varepsilon_{\boldsymbol{nk}}} \tag{4}$$

($\alpha = x, y, z$; ρ_0 is the equilibrium Bose-Einstein distribution; $\tau_{\boldsymbol{nk}}$ is the relaxation time; $\boldsymbol{v}_{\boldsymbol{nk}} = \hbar^{-1} \partial \varepsilon_{\boldsymbol{nk}}/\partial \boldsymbol{k}$ is the magnon velocity; V is the sample volume). For $\boldsymbol{\Omega}_{\boldsymbol{nk}} = 0$ or $\mathcal{B} = 0$, they reduce to [28,29]

$$L_{i,\alpha\alpha} = \frac{(g\mu_\mathrm{B})^{2-i}}{V} \sum_{\boldsymbol{nk}} \tau_{\boldsymbol{nk}} (-\xi_{\boldsymbol{nk}})^{2-i} \varepsilon_{\boldsymbol{nk}}^{i} v_{\alpha,\boldsymbol{nk}}^2 \left(-\frac{\partial \rho_0}{\partial \varepsilon} \right) \Bigg|_{\varepsilon_{\boldsymbol{nk}}}. \tag{5}$$

The respective magnon transport phenomena are depicted in the first row of Fig. 1 [panels (a)–(d)]. A similar expression is found for the normal (N) Hall-type contribution [19,27,28,30,31],

$$L_{i,xy}^\mathrm{N} = \frac{(g\mu_\mathrm{B})^{3-i}}{\hbar V} \frac{E'}{c^2} \tau^2 \sum_{\boldsymbol{nk}} (-\xi_{\boldsymbol{nk}})^{3-i} \varepsilon_{\boldsymbol{nk}}^{i} v_{x,\boldsymbol{nk}} \times \left(v_{y,\boldsymbol{nk}} \frac{\partial v_{y,\boldsymbol{nk}}}{\partial k_x} - v_{x,\boldsymbol{nk}} \frac{\partial v_{y,\boldsymbol{nk}}}{\partial k_y} \right) \frac{\partial \rho_0}{\partial \varepsilon} \Bigg|_{\varepsilon_{\boldsymbol{nk}}} \tag{6}$$

for which we assume cubic symmetry and a constant relaxation time [Figs. 1(e)–1(h)]. E' denotes an electric-field gradient. Finally, we obtain for the intrinsic anomalous (A) off-diagonal elements [19,27,32–40],

$$L_{i,xy}^\mathrm{A} = -\frac{(g\mu_\mathrm{B})^{2-i}}{\hbar V} (k_\mathrm{B} T)^i \sum_{\boldsymbol{nk}} (-\xi_{\boldsymbol{nk}})^{2-i} \Omega_{z,\boldsymbol{nk}} c_i[\rho_0(\varepsilon_{\boldsymbol{nk}})], \tag{7}$$

with $c_i[\rho_0(\varepsilon_{\boldsymbol{nk}})]$ given in the Supplemental Material [19]. Out of the four anomalous phenomena [Figs. 1(i)–1(l)] only the magnon Righi-Leduc effect [panel (l)]—also called the thermal magnon Hall effect—has been measured [41–43].

Equations (4)–(7), which are valid for *any* EA magnet, contain $-\xi_{\boldsymbol{nk}}$. This leads to fundamentally different transport phenomena in ferromagnets, antiferromagnets, and ferrimagnets as we demonstrate in the following.

Ferromagnets. Magnon transport in ferromagnets is analogous to electron transport since $\xi_{\boldsymbol{nk}} = -1$ [44]: There is a single type of "charge". At low temperatures, only the lowest magnon band contributes to transport. We assume a parabolic band $\varepsilon_{\boldsymbol{k}} = Ak^2 + \Delta\varepsilon$, where A is the spin-wave stiffness and $\Delta\varepsilon$ is the magnon gap (due to a constant magnetic field and the EA anisotropy). Setting $\tau_{\boldsymbol{k}} = \tau$ as constant in Eq. (5), we obtain [19]

$$L_{i,\alpha\alpha}(T, \Delta\varepsilon) \approx \frac{(g\mu_\mathrm{B})^{2-i} \tau}{3\pi^2 \hbar^2 \sqrt{A}} (k_\mathrm{B} T)^{3/2+i} F_i(x_0), \tag{8}$$

with $F_i(x_0)$ given in the Supplemental Material [19]; $x_0 = \Delta\varepsilon/(k_\mathrm{B} T)$. For $\Delta\varepsilon = 0$ we find $\sigma_{\alpha\alpha}, \Upsilon_{\alpha\alpha} \propto T^{3/2}$, $\kappa_{\alpha\alpha} \propto T^{5/2}$, and $S \approx 1.284 \times k_\mathrm{B}/(g\mu_\mathrm{B})$ in accordance with Ref. [46]. $S \propto x_0$ for $x_0 \to \infty$; setting $\Delta\varepsilon = g\mu_\mathrm{B} B_z$, this translates into $S \sim B_z/T$, which is in line with Ref. [21]; this behavior was also observed in computer simulations [22]. Moreover, a magnon Wiedemann-Franz law $\mathcal{L} = \kappa_{\alpha\alpha}/(T\sigma_{\alpha\alpha})$ [21] is found with the magnon Lorenz number $\mathcal{L} = [F_2/F_0 - (F_1/F_0)^2] k_\mathrm{B}^2/(g\mu_\mathrm{B})^2$. The numerical factor evaluates to $5/2$ in the limit $\Delta\varepsilon/(k_\mathrm{B} T) \to \infty$ [47].

We predict the magnon counterparts to the normal Hall-effect family [second row in Fig. 1; see also Ref. [16] for the normal magnon Hall effect; Fig. 1(e)]. For parabolic bands, Eq. (6) establishes $L_{i,xy}^\mathrm{N} \approx \omega_\mathrm{c} \tau L_{i,xx}$ ($\omega_\mathrm{c}\tau \ll 1$) [19] where $\omega_\mathrm{c} = |e|\mathcal{B}/m^\star = g\mu_\mathrm{B} E'/(m^\star c^2)$ is the magnon cyclotron frequency [$m^\star = \hbar^2/(2A)$ is the effective mass] with $L_{i,xx}$ given by Eq. (8). To obtain $\omega_\mathrm{c}\tau = 10^{-2}$—e.g., a magnon Nernst signal [$\Upsilon_{1,xy}^\mathrm{N}$, Fig. 1(g)] one-hundredth of a magnon Seebeck signal without E' [$\Upsilon_{1,xx}$, Fig. 1(c)]—gigantic gradients $E' \approx 10^{17}$ V/m^2 are necessary [48]. In the quantum limit the dual magnetic field causes Landau-level condensation of magnons [23].

The bottom row of Fig. 1 depicts anomalous transport effects caused by the Berry curvature $\boldsymbol{\Omega}_{\boldsymbol{nk}}$, e.g., in topological magnon insulators (TMIs) [22,49–68] or magnon Weyl semimetals (MWSs) [69–72]. Here, either the Dzyaloshinskii-Moriya interaction (DMI) [49,73,74] or a scalar spin chirality [63–65,69] breaks the time-reversal symmetry of the free-magnon Hamiltonian.

The intrinsic anomalous conductivities are given as $\boldsymbol{k}$-space integrals over the (weighted) Berry curvature. Equation (7)

mainly agrees with Refs. [35–39], however we point out a crucial difference: κ_{xy} is not only given by the nominal part $\kappa_{xy}^{\mathrm{nom}} = L_{2,xy}^{\mathrm{A}}/T$ but corrected by $\kappa_{xy}^{\mathrm{cor}} = -L_1 L_0^{-1} L_1/T|_{xy}$. This magnetothermal correction is attributed to the dual electric field which builds up upon magnon accumulation; it counteracts the temperature gradient. Although such a correction is usually neglected for electrons, there is no reason for $\kappa_{xy}^{\mathrm{cor}} \ll \kappa_{xy}^{\mathrm{nom}}$ for magnons [75]. Thus, κ_{xy} is determined by both the Berry curvature integrals in Eq. (7) and by the diagonal components of L_0 and L_1: It is *not purely intrinsic* as it depends on the relaxation time [cf. Eq. (5)] [19,76]. Since σ_{xy} and Υ_{xy} do not, they are better suited than κ_{xy} to study the topological properties of magnons. This calls for measurements of the anomalous magnon Hall, Ettingshausen, and Nernst effects in, e.g., $Lu_2V_2O_7$ [41] and Cu(1,3-benzenedicarboxylate) [43]. Quantized transverse conductivities are not expected in contrast to electrons.

The recently discovered MWSs [69] (e.g., $Lu_2V_2O_7$ [70,72]) host linearly dispersive Weyl cones, similar to their electronic counterparts [77]. Electronic Weyl semimetals are known to exhibit a negative magnetoresistance due to the chiral anomaly (the electronic conductivity increases as $\sigma_{xx} \propto B^2$) [6–8,78,79]. From Eq. (4) we predict that there is a similar effect in MWSs: Aligning the dual electromagnetic fields ($\boldsymbol{\mathcal{E}} \parallel \boldsymbol{\mathcal{B}} \parallel \hat{\boldsymbol{x}}$) leads to $\sigma_{xx} \propto E'^2$ [19]; see also Refs. [72,80,81]. However, two obstacles are identified: a gigantic E' is necessary [82], and the contribution of the Weyl points to transport is significantly diminished by the energy derivative of the Bose-Einstein distribution function $\partial\rho_0/\partial\varepsilon|_{\varepsilon_{\mathrm{W}}}$ at the energy ε_{W} of the Weyl points.

Antiferromagnets. The spin-degenerate magnon bands of antiferromagnets host positively and negatively dually charged magnons ($\pm q$), which respond exactly oppositely to the dual electromagnetic fields. Thus, all transport tensor elements proportional to an odd power of $\xi_{n\boldsymbol{k}}$ vanish.

A dual electric-field $\boldsymbol{\mathcal{E}}$ causes counterpropagating magnon currents: There is a net magnetization current but no particle or heat current [Fig. 2(a)]. Thus, there is no magnon Peltier effect in antiferromagnets, which agrees with Eq. (5): $L_{1,\alpha\alpha} \propto \xi_{n\boldsymbol{k}}$. Similarly, there is no magnon Seebeck effect [83–87]: A temperature gradient causes a net particle/heat current containing in equal parts positively and negatively charged magnons [Fig. 2(b)]. This finding satisfies Onsager's reciprocity relation. Magnon Ohm's and Fourier's laws [Figs. 1(a) and 1(d)] remain intact [88] because $L_{0,\alpha\alpha} \propto \xi_{n\boldsymbol{k}}^2$ and $L_{2,\alpha\alpha} \propto \xi_{n\boldsymbol{k}}^0$.

If simultaneously dual $\boldsymbol{\mathcal{E}}$ and $\boldsymbol{\mathcal{B}}$ fields are applied ($\boldsymbol{\mathcal{E}} \perp \boldsymbol{\mathcal{B}}$), there is no net transverse spin current (no normal magnon Hall effect): $L_{0,xy}^{\mathrm{N}} \propto \xi_{n\boldsymbol{k}}^3$ [cf. Eq. (6), Fig. 2(c)]. Similarly, there is no normal magnon Righi-Leduc effect ($L_{2,xy}^{\mathrm{N}} \propto \xi_{n\boldsymbol{k}}$): Although the temperature gradient drives all magnons in the same direction, $\boldsymbol{\mathcal{B}}$ separates them by their charge [Fig. 2(d)], in agreement with Ref. [89].

Concerning anomalous transport, we recall that the Berry curvature of spin-degenerate bands and, thus, the anomalous velocities of the two magnon species are exactly opposite. Consequently, $L_{0,xy}^{\mathrm{A}} = L_{2,xy}^{\mathrm{A}} = 0$ [cf. Eq. (7)]; in agreement with Refs. [89–91], there can only be an anomalous magnon Nernst/Ettingshausen effect, whose signatures were found in experiments [92]. Compared to the normal effects, the Berry curvature has taken over the role of the species-dependent

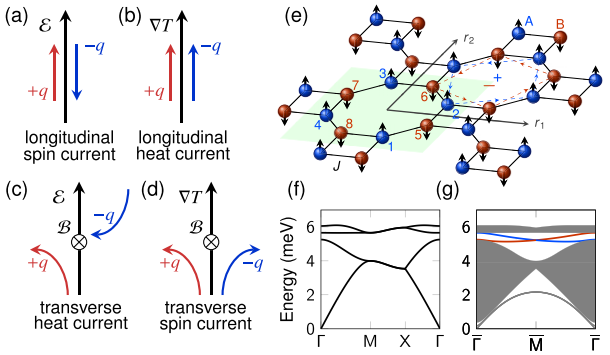

FIG. 2. (a)–(d) Electron-magnon duality interpretation of magnon transport in collinear EA antiferromagnets for selected combinations of forces. The different magnon species (spin up vs spin down) are identified by their dual charge $\pm q$. They "feel" a dynamical Lorentz force due to the dual electromagnetic fields $\boldsymbol{\mathcal{E}}$ and $\boldsymbol{\mathcal{B}}$ and a statistical force due to a temperature gradient $\boldsymbol{\nabla} T$. The response (not in the dual picture) is indicated (spin or a particle/heat current). (e)–(g) $\mathbb{Z}_2$ topological magnon insulator. (e) Square-octagon lattice with eight basis sites and magnetic Néel order. Positive DMI is assumed within octagons for counterclockwise direction (the dashed lines). (f) Spin-degenerate magnon bulk bands with a band gap; $DS = 0.05$ meV, $JS = -1$ meV. (g) Slab magnon dispersion with helical edge magnons (red and blue).

force $q_{n\boldsymbol{k}} \boldsymbol{v}_{n\boldsymbol{k}} \times \boldsymbol{\mathcal{B}}$. This is reminiscent of the interpretation of spin-orbit interaction as a spin-dependent intrinsic magnetic field. Thus, anomalous transport in antiferromagnets is the counterpart to the spin Hall physics of electrons [89–91].

This relation is underlined by the existence of $\mathbb{Z}_2$ topological magnon phases in Néel antiferromagnets, e.g., on the square-octagon lattice [Fig. 2(e)]. The minimal spin Hamiltonian $H = -J \sum_{\langle ij \rangle} \hat{\boldsymbol{S}}_i \cdot \hat{\boldsymbol{S}}_j + \sum_{\langle\langle ij \rangle\rangle} D_{ij} \hat{\boldsymbol{z}} \cdot (\boldsymbol{S}_i \times \boldsymbol{S}_j)$ contains an antiferromagnetic exchange between nearest ($J < 0$) and DMI between second-nearest neighbors in the octagons [the dashed lines in Fig. 2(e)]; $D_{ij} > 0$ in the counterclockwise direction. Within spin-wave theory eight magnon bulk bands are found [Fig. 2(f)], whose spin degeneracy is protected by the combined symmetry of time-reversal and inversion symmetries [93]. Nonzero DMI opens up a band gap, allowing for calculating the Chern numbers $C_{\uparrow(\downarrow)}$ of each spin sector for the bands below the gap. Since the DMI acts between spins of the same sublattice and the sublattices have opposite magnetizations ["±" in Fig. 2(e)] $C_\uparrow = -C_\downarrow$. The $\mathbb{Z}_2$ index $\nu = (C_\uparrow - C_\downarrow)/2$ equals 1, indicating a topologically nontrivial situation. This is verified by helical edge magnons as found in slab calculations [Fig. 2(g)]: The propagation direction of the edge magnons is locked to their spin. Such helical edge states are also found in the quantum (spin) Hall limit of antiferromagnets [89], relying on an electric-field gradient.

Ferrimagnets. Like in antiferromagnets, the magnons in ferrimagnets carry opposite charges, but the degeneracy of the bands is lifted. Thus, transport coefficients that vanish in antiferromagnets can *change sign* in ferrimagnets: If an energetically lower mode with $\xi_{n\boldsymbol{k}} > 0$ has a small bandwidth, its contribution to transport can be exceeded by a higher mode with $\xi_{n\boldsymbol{k}} < 0$ and a larger bandwidth upon increasing

temperature. This is in line with Ref. [94] in which sign changes in the spin Seebeck signal were discussed.

Following the work of Sodemann and Fu on nonlinear electronic transport [95], an additional observation regarding *nonlinear magnon transport* in ferrimagnets can be made. The nonlinear (NL) magnetization current density $J_{\mathrm{NL},\alpha} = \chi_{\alpha\beta\gamma}(\partial_\beta B_z)(\partial_\gamma B_z)$ contains $\chi_{\alpha\beta\gamma} = \epsilon_{\alpha\delta\gamma}(g\mu_\mathrm{B})^3\tau D_{\beta\delta}/\hbar^2$ (τ is the constant relaxation time; $\epsilon_{\alpha\delta\gamma}$ is the Levi-Civita symbol) in which

$$D_{\alpha\beta} = \frac{1}{V}\sum_{n,\boldsymbol{k}}(-\xi_{n\boldsymbol{k}})^3\frac{\partial\Omega_{\beta,n\boldsymbol{k}}}{\partial k_\alpha}\rho_0(\varepsilon_{n\boldsymbol{k}}) \tag{9}$$

is the "Berry curvature dipole tensor" [19,95]. Although the integrals in Eq. (7) are zero, if $\boldsymbol{\Omega}_{n\boldsymbol{k}} = -\boldsymbol{\Omega}_{n,-\boldsymbol{k}}$ holds, this is not necessarily the case for $D_{\alpha\beta}$. Thus, time-reversal symmetric systems with broken parity symmetry might show nonlinear transverse transport (symmetry requirements for a nonzero $D_{\alpha\beta}$ are discussed in Ref. [95]).

Here, we concentrate on special two-dimensional ferrimagnets and demonstrate that these fulfill the above requirements. In two dimensions, $D_{\alpha\beta}$ reduces to a vector $\boldsymbol{D}$ (only $\partial\Omega_{z,n\boldsymbol{k}}/\partial k_\alpha$ for $\alpha = x,y$ can be nonzero), and the nonlinear current reads $\boldsymbol{J}_\mathrm{NL} = (g\mu_\mathrm{B})^3\tau\hat{\boldsymbol{z}}\times(\boldsymbol{\nabla}B_z)[\boldsymbol{D}\cdot(\boldsymbol{\nabla}B_z)]/\hbar^2$ [95]. Thus, $\boldsymbol{\nabla}B_z$ parallel to $\boldsymbol{D}$ causes a *nonlinear* magnon current orthogonal to $\boldsymbol{\nabla}B_z$. For $\boldsymbol{\nabla}B_z \perp \boldsymbol{D}$ there is no transverse current, which is fundamentally different from *linear* anomalous currents which are independent of the direction of $\boldsymbol{\nabla}B_z$.

For a proof of principle, we consider a two-dimensional two-sublattice "pseudo" ferrimagnet: there are two spin species with lengths S_A and S_B, but they are *ferro*magnetically coupled. Our model spin Hamiltonian $H = -J\sum_{\langle ij\rangle}\hat{\boldsymbol{S}}_i\cdot\hat{\boldsymbol{S}}_j - K\sum_i\hat{S}^2_{z,i}$ contains nearest-neighbor exchange interaction $J > 0$ and single-ion anisotropy $K > 0$. After a Holstein-Primakoff transformation [96] about the polarized ground state the bilinear spin-wave Hamiltonian reads $\sum_{\boldsymbol{k}}\boldsymbol{\psi}^\dagger(\boldsymbol{k})\mathsf{H}(\boldsymbol{k})\boldsymbol{\psi}(\boldsymbol{k})$. The two-level Hamilton matrix in the basis $\boldsymbol{\psi}(\boldsymbol{k}) = (a_{\boldsymbol{k},\mathrm{A}}, a_{\boldsymbol{k},\mathrm{B}})^\mathrm{T}$ ($a_{\boldsymbol{k},\mathrm{A}}$ is the annihilation operator) reads $\mathsf{H}(\boldsymbol{k}) = f_0\sigma_0 + \boldsymbol{f}(\boldsymbol{k})\cdot\boldsymbol{\sigma}$ with $f_0 = Jz(S_\mathrm{A}+S_\mathrm{B})/2 + K$,

$$\boldsymbol{f}(\boldsymbol{k}) = \begin{pmatrix} -J\sqrt{S_\mathrm{A}S_\mathrm{B}}\sum_{i=1}^z\cos(\boldsymbol{k}\cdot\boldsymbol{\delta}_i) \\ J\sqrt{S_\mathrm{A}S_\mathrm{B}}\sum_{i=1}^z\sin(\boldsymbol{k}\cdot\boldsymbol{\delta}_i) \\ Jz(S_\mathrm{B}-S_\mathrm{A})/2 \end{pmatrix}$$

($\sigma_0 = \mathbf{1}$, $\boldsymbol{\sigma}$ is the vector of Pauli matrices, $\boldsymbol{\delta}_i$'s are vectors to the z nearest neighbors). The Berry curvature $\Omega_n(\boldsymbol{k}) = (-1)^n\boldsymbol{f}\cdot(\partial_{k_x}\boldsymbol{f}\times\partial_{k_y}\boldsymbol{f})/(2f^3)$ ($n = 1,2$) obeys $\Omega_n(\boldsymbol{k}) = -\Omega_n(-\boldsymbol{k})$ as well as $\Omega_1(\boldsymbol{k}) = -\Omega_2(\boldsymbol{k})$. Either $S_\mathrm{A} = S_\mathrm{B}$ (ferromagnet) or $f_2(\boldsymbol{k}) = 0$ (lattice sites are centers of inversion) lead to $\Omega_n(\boldsymbol{k}) = 0$.

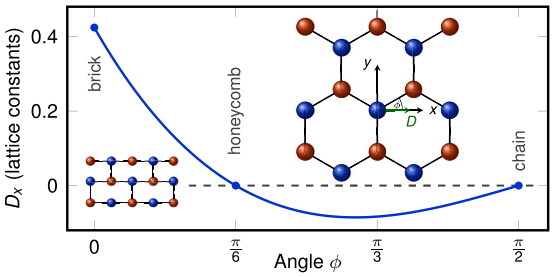

FIG. 3. Nonlinear anomalous magnon Hall effect in ferrimagnets. Berry curvature dipole vector $\boldsymbol{D}$ vs angle ϕ; only D_x is nonzero. For $\phi = 0,\pi/6,\pi/2$, a brick (the left inset), a honeycomb (the right inset), and a chain lattice are formed, respectively. Parameters read $S_\mathrm{A} = 1$, $S_\mathrm{B} = 3/2$, $k_\mathrm{B}T = J$, $K = 0.05J$.

We now evaluate $\boldsymbol{D}$ for selected lattices (Fig. 3). We start with the honeycomb lattice (the right inset), having in mind ferrimagnetic Fe(II)Fe(III) bimetallic oxalates [97]. The bond centers are centers of inversion, but the sites are not. Thus, the DMI between nearest neighbors vanishes, and $\Omega_{n\boldsymbol{k}} = -\Omega_{n,-\boldsymbol{k}}$ holds [98]; there is *no linear anomalous transport*. The threefold rotational symmetry renders $\boldsymbol{D} = 0$ [95]. It can be broken by strain, which is parametrized by an angle ϕ (the right inset). For $\phi \neq \pi/6$ or $\pi/2$, $\boldsymbol{D}$ is nonzero and orthogonal to the mirror line (the y axis [100]; $D_x \neq 0$, $D_y = 0$). Compressive ($\phi < \pi/6$) and tensile strain ($\phi > \pi/6$) cause opposite orientations of $\boldsymbol{D}$ and, hence, of the nonlinear current. $\boldsymbol{D}$ is maximal for the brick lattice ($\phi = 0$, the left small inset).

Summary. We presented a theory to derive magnon transport phenomena via a duality shortcut from the electronic counterparts. Besides the longitudinal magnon transport effects, it captures effects that are related to the Berry curvature and provides a correction to the transverse thermal conductivity of the anomalous magnon Righi-Leduc effect. On top of this, it describes modern phenomena, e.g., the family of normal magnon Hall-type effects and a negative magnon magnetoresistance in magnon Weyl semimetals and predicts new effects, such as a nonlinear anomalous magnon Hall effect in inversion-symmetry broken magnets with low symmetry, e.g., in ferrimagnets on the brick lattice.

Acknowledgments. A.M. acknowledges fruitful discussions with V. Basso, A. Kovalev, and A. Johansson. We thank K. Nakata for bringing an independent study [89] on magnon transport and the quantum spin Hall effect of magnons in antiferromagnets to our attention. This Rapid Communication was supported by Grants No. SPP 1666 and No. SPP 1538 of Deutsche Forschungsgemeinschaft (DFG).

[1] L. Landau, Z. Phys. **64**, 629 (1930).
[2] E. H. Hall, Am. J. Math. **2**, 287 (1879).
[3] E. Hall, Philosophical Magazine Series 5 **12**, 157 (1881).
[4] N. Nagaosa, J. Sinova, S. Onoda, A. H. MacDonald, and N. P. Ong, Rev. Mod. Phys. **82**, 1539 (2010).
[5] D. Xiao, M.-C. Chang, and Q. Niu, Rev. Mod. Phys. **82**, 1959 (2010).
[6] H. Nielsen and M. Ninomiya, Phys. Lett. B **130**, 389 (1983).
[7] D. T. Son and B. Z. Spivak, Phys. Rev. B **88**, 104412 (2013).
[8] A. A. Burkov, J. Phys.: Condens. Matter **27**, 113201 (2015).
[9] G. Sundaram and Q. Niu, Phys. Rev. B **59**, 14915 (1999).
[10] M. V. Berry, Proc. R. Soc. London, Ser. A **392**, 45 (1984).
[11] J. Zak, Phys. Rev. Lett. **62**, 2747 (1989).
[12] Y. Aharonov and A. Casher, Phys. Rev. Lett. **53**, 319 (1984).

[13] J. Anandan, Phys. Lett. A **138**, 347 (1989).
[14] S. M. Al-Jaber, X. Zhu, and W. C. Henneberger, Eur. J. Phys. **12**, 268 (1991).
[15] M. Ericsson and E. Sjöqvist, Phys. Rev. A **65**, 013607 (2001).
[16] F. Meier and D. Loss, Phys. Rev. Lett. **90**, 167204 (2003).
[17] S. Dulat and K. Ma, Phys. Rev. Lett. **108**, 070405 (2012).
[18] T. Choi and S. Y. Cho, Phys. Rev. Lett. **112**, 158901 (2014).
[19] See Supplemental Material at http://link.aps.org/supplemental/10.1103/PhysRevB.97.140401 for details of the arguments and derivations.
[20] B. Liao, J. Zhou, and G. Chen, Phys. Rev. Lett. **113**, 025902 (2014).
[21] K. Nakata, P. Simon, and D. Loss, Phys. Rev. B **92**, 134425 (2015).
[22] A. Mook, J. Henk, and I. Mertig, Phys. Rev. B **94**, 174444 (2016).
[23] K. Nakata, J. Klinovaja, and D. Loss, Phys. Rev. B **95**, 125429 (2017).
[24] A. Mook, B. Göbel, J. Henk, and I. Mertig, Phys. Rev. B **95**, 020401 (2017).
[25] K.-S. Kim, H.-J. Kim, and M. Sasaki, Phys. Rev. B **89**, 195137 (2014).
[26] R. Lundgren, P. Laurell, and G. A. Fiete, Phys. Rev. B **90**, 165115 (2014).
[27] G. Sharma, P. Goswami, and S. Tewari, Phys. Rev. B **93**, 035116 (2016).
[28] J. Callaway, *Quantum Theory of the Solid State* (Academic, London, 1974).
[29] A. A. Kovalev and Y. Tserkovnyak, Europhys. Lett. **97**, 67002 (2012).
[30] H. Jones and C. Zener, Proc. R. Soc. London, Ser. A **145**, 268 (1934).
[31] R. G. Chambers, Proc. Phys. Soc., London, Sect. A **65**, 458 (1952).
[32] D. Xiao, Y. Yao, Z. Fang, and Q. Niu, Phys. Rev. Lett. **97**, 026603 (2006).
[33] D. L. Bergman and V. Oganesyan, Phys. Rev. Lett. **104**, 066601 (2010).
[34] T. Yokoyama and S. Murakami, Phys. Rev. B **83**, 161407 (2011).
[35] R. Matsumoto and S. Murakami, Phys. Rev. B **84**, 184406 (2011).
[36] R. Matsumoto and S. Murakami, Phys. Rev. Lett. **106**, 197202 (2011).
[37] R. Matsumoto, R. Shindou, and S. Murakami, Phys. Rev. B **89**, 054420 (2014).
[38] H. Lee, J. H. Han, and P. A. Lee, Phys. Rev. B **91**, 125413 (2015).
[39] J. H. Han and H. Lee, J. Phys. Soc. Jpn. **86**, 011007 (2017).
[40] S. Murakami and A. Okamoto, J. Phys. Soc. Jpn. **86**, 011010 (2017).
[41] Y. Onose, T. Ideue, H. Katsura, Y. Shiomi, N. Nagaosa, and Y. Tokura, Science **329**, 297 (2010).
[42] T. Ideue, Y. Onose, H. Katsura, Y. Shiomi, S. Ishiwata, N. Nagaosa, and Y. Tokura, Phys. Rev. B **85**, 134411 (2012).
[43] M. Hirschberger, R. Chisnell, Y. S. Lee, and N. P. Ong, Phys. Rev. Lett. **115**, 106603 (2015).
[44] We neglect dipolar interactions and magnon "squeezing" [45].
[45] A. Kamra, U. Agrawal, and W. Belzig, Phys. Rev. B **96**, 020411 (2017).
[46] V. Basso, E. Ferraro, and M. Piazzi, Phys. Rev. B **94**, 144422 (2016).
[47] This result depends strongly on the dimension d and the relaxation time: Supposing $\tau \propto k^{-n}$, the prefactor reads $(2 + d - n)/2$.
[48] We used $m^\star = 2.5 \times 10^{-28}$ kg and $\tau = 10^{-7}$ s.
[49] H. Katsura, N. Nagaosa, and P. A. Lee, Phys. Rev. Lett. **104**, 066403 (2010).
[50] L. Zhang, J. Ren, J.-S. Wang, and B. Li, Phys. Rev. B **87**, 144101 (2013).
[51] R. Shindou, R. Matsumoto, S. Murakami, and J.-i. Ohe, Phys. Rev. B **87**, 174427 (2013)
[52] A. Mook, J. Henk, and I. Mertig, Phys. Rev. B **89**, 134409 (2014).
[53] A. Mook, J. Henk, and I. Mertig, Phys. Rev. B **90**, 024412 (2014).
[54] X. Cao, K. Chen, and D. He, J. Phys.: Condens. Matter **27**, 166003 (2015).
[55] A. Mook, J. Henk, and I. Mertig, Phys. Rev. B **91**, 174409 (2015).
[56] A. Mook, J. Henk, and I. Mertig, Phys. Rev. B **91**, 224411 (2015).
[57] R. Chisnell, J. S. Helton, D. E. Freedman, D. K. Singh, R. I. Bewley, D. G. Nocera, and Y. S. Lee, Phys. Rev. Lett. **115**, 147201 (2015).
[58] A. L. Chernyshev and P. A. Maksimov, Phys. Rev. Lett. **117**, 187203 (2016).
[59] B. Xu, T. Ohtsuki, and R. Shindou, Phys. Rev. B **94**, 220403 (2016).
[60] S. A. Owerre, J. Appl. Phys. **120**, 043903 (2016).
[61] S. A. Owerre, J. Phys.: Condens. Matter **28**, 386001 (2016).
[62] S. A. Owerre, Phys. Rev. B **94**, 094405 (2016).
[63] S. A. Owerre, J. Phys.: Condens. Matter **28**, 47LT02 (2016).
[64] S. A. Owerre, Phys. Rev. B **95**, 014422 (2017).
[65] S. A. Owerre, J. Phys.: Condens. Matter **29**, 03LT01 (2017).
[66] S. A. Owerre, Europhys. Lett. **117**, 37006 (2017).
[67] P. Laurell and G. A. Fiete, Phys. Rev. Lett. **118**, 177201 (2017).
[68] X. S. Wang, Y. Su, and X. R. Wang, Phys. Rev. B **95**, 014435 (2017).
[69] F.-Y. Li, Y.-D. Li, Y. B. Kim, L. Balents, Y. Yu, and G. Chen, Nat. Commun. **7**, 12691 (2016).
[70] A. Mook, J. Henk, and I. Mertig, Phys. Rev. Lett. **117**, 157204 (2016).
[71] A. Mook, J. Henk, and I. Mertig, Phys. Rev. B **95**, 014418 (2017).
[72] Y. Su, X. S. Wang, and X. R. Wang, Phys. Rev. B **95**, 224403 (2017).
[73] I. Dzyaloshinsky, J. Phys. Chem. Solids **4**, 241 (1958).
[74] T. Moriya, Phys. Rev. **120**, 91 (1960).
[75] References [21,23] show that only the inclusion of the correction term leads to a magnon Wiedemann-Franz law [19].
[76] With the sign change in κ_{xy} in the TMI Cu(1,3-benzenedicarboxylate) in mind [43], the correction term is expected to be significant.
[77] X. Wan, A. M. Turner, A. Vishwanath, and S. Y. Savrasov, Phys. Rev. B **83**, 205101 (2011).

[78] X. Huang, L. Zhao, Y. Long, P. Wang, D. Chen, Z. Yang, H. Liang, M. Xue, H. Weng, Z. Fang *et al.*, Phys. Rev. X **5**, 031023 (2015).
[79] C.-L. Zhang, S.-Y. Xu, I. Belopolski, Z. Yuan, Z. Lin, B. Tong, G. Bian, N. Alidoust, C.-C. Lee, S.-M. Huang *et al.*, Nat. Commun. **7**, 10735 (2016).
[80] Y. Su and X. R. Wang, Phys. Rev. B **96**, 104437 (2017).
[81] References [72,80] consider the chiral anomaly of Weyl magnons in the quantum limit: The magnon conductance increases with E'. This difference for our result is in analogy to electrons: $\sigma_{xx} \propto B^2$ in the semiclassical [7] and $\propto B$ in the quantum limits [6].
[82] $E' = 7.7 \times 10^{20}$ V/m^2 is necessary to obtain $|\mathcal{B}| = 1$ T.
[83] Y. Ohnuma, H. Adachi, E. Saitoh, and S. Maekawa, Phys. Rev. B **87**, 014423 (2013).
[84] S. M. Rezende, R. L. Rodríguez-Suárez, and A. Azevedo, Phys. Rev. B **93**, 014425 (2016).
[85] S. M. Rezende, R. L. Rodríguez-Suárez, and A. Azevedo, Phys. Rev. B **93**, 054412 (2016).
[86] S. Seki, T. Ideue, M. Kubota, Y. Kozuka, R. Takagi, M. Nakamura, Y. Kaneko, M. Kawasaki, and Y. Tokura, Phys. Rev. Lett. **115**, 266601 (2015).
[87] S. M. Wu, W. Zhang, A. KC, P. Borisov, J. E. Pearson, J. S. Jiang, D. Lederman, A. Hoffmann, and A. Bhattacharya, Phys. Rev. Lett. **116**, 097204 (2016).
[88] A. Brataas, H. Skarsvåg, E. G. Tveten, and E. Løhaugen Fjærbu, Phys. Rev. B **92**, 180414 (2015).
[89] K. Nakata, S. K. Kim, J. Klinovaja, and D. Loss, Phys. Rev. B **96**, 224414 (2017).
[90] R. Cheng, S. Okamoto, and D. Xiao, Phys. Rev. Lett. **117**, 217202 (2016).
[91] V. A. Zyuzin and A. A. Kovalev, Phys. Rev. Lett. **117**, 217203 (2016).
[92] Y. Shiomi, R. Takashima, and E. Saitoh, Phys. Rev. B **96**, 134425 (2017).
[93] K. Li, C. Li, J. Hu, Y. Li, and C. Fang, Phys. Rev. Lett. **119**, 247202 (2017).
[94] S. Geprägs, A. Kehlberger, F. D. Coletta, Z. Qiu, E.-J. Guo, T. Schulz, C. Mix, S. Meyer, A. Kamra, M. Althammer *et al.*, Nat. Commun. **7**, 10452 (2016).
[95] I. Sodemann and L. Fu, Phys. Rev. Lett. **115**, 216806 (2015)
[96] T. Holstein and H. Primakoff, Phys. Rev. **58**, 1098 (1940).
[97] R. S. Fishman and F. A. Reboredo, Phys. Rev. B **77**, 144421 (2008).
[98] This is the magnon version of Haldane's model [99] with asymmetric on-site potentials but without textured magnetic flux.
[99] F. D. M. Haldane, Phys. Rev. Lett. **61**, 2015 (1988).
[100] The mirror symmetry is the only symmetry compatible with $\boldsymbol{D} \neq 0$ [95].